An investigation of three-body effects in intermolecular forces. II. Far-infrared vibration–rotation–tunneling laser spectroscopy of Ar_2HCl

M. J. Elrod, D. W. Steyert, and R. J. Saykally
Department of Chemistry, University of California, Berkeley, California 94720

(Received 16 April 1991; accepted 30 May 1991)

A second Ar_2HCl intermolecular vibration–rotation band centered at 37.2 cm^{-1} has been measured and assigned as a *b*-type transition originating from the ground state. Nuclear hyperfine splittings were resolved for both chlorine isotopes. The rotational constants determined from the data indicate coupling between an Ar–Ar stretching or bending coordinate and the Ar_2–HCl vibrational coordinates. As a result of this particular vibrational motion, $Ar_2H\,^{35}Cl$ undergoes an axis-switching transition while the $Ar_2H\,^{37}Cl$ isotope does not. In addition, the measured hyperfine projections indicate the possibility of coupling between the Ar_2–HCl stretching and bending modes, preventing an absolute vibrational assignment. These results indicate that the "reversed adiabatic" approximation employed by Hutson, Beswick, and Halberstadt in their theoretical study of Ar_2HCl [J. Chem. Phys. **90**, 1337 (1989)] is not appropriate for the complicated intramolecular dynamics presently observed in this system.

INTRODUCTION

Throughout the history of the study of intermolecular forces, many-body effects have been invoked to explain a wide range of "anomalous" physical properties. For instance, with the exception of helium, the lattice structures of rare-gas crystals are observed to be face-centered cubic, while molecular-dynamics calculations utilizing the most accurate pair potential functions predict a hexagonal-close-packed structure. Several researchers have claimed that three-body forces are responsible for this subtle change in relative crystal binding energies, but no direct proof exists to support this assumption.[1] Many-body effects have also been implicated in such subjects ranging from base-pairing stabilities in DNA[2] to gas–surface interactions.[3,4]

The experimental and theoretical methods previously used to address the effects of many-body forces are, by modern standards, quite crude. Classical experiments such as transport property and gas imperfection studies have been used to examine many-body effects in rare-gas systems, but the quality of the information extracted from such efforts is extremely limited. Consequently, even for such extensively studied systems as the rare gases, the only concrete conclusions resulting from such experiments are the *existence* of many-body forces rather than information about the *form* of these forces. The Axilrod–Teller (AT) triple-dipole term[5]—the three-body correction to the dispersion energies—has been used with little discretion to fit experimental data to model potential-energy functions. Recent *ab initio* calculations indicate that the apparent success of the AT term may only be a fortuitious coincidence, as the three-body exchange energies are estimated to be of the same magnitude and opposite sign as the AT energies, suggesting a complicated cancellation of additional many-body terms.[6] In their recent *ab initio* study of Ar_2H_2O, Chalasinski, Szczesniak, and Scheiner conclude that the existence of large many-body effects are unlikely because of this cancellation of the leading many-body exchange and dispersion terms, but that "none of the three-body contributions is negligible and approximation of the total three-body effect by any one of them would be improper."[7]

In recent years, new spectroscopic techniques have been developed in order to study intermolecular forces with much greater detail than was possible with previous experiments. Several microwave spectroscopy groups have now provided very detailed information on the ground states of literally hundreds of van der Waals clusters, including recent studies of polymeric van der Waals molecules (cf. Refs. 8–13). However, these studies provide limited information on the intermolecular potential, as the ground-state wave functions are usually localized near the van der Waals minimum. The determination of an anisotropic potential-energy surface for ArHCl (Ref. 14) from precise far-infrared (FIR) laser spectroscopy measurements of van der Waals stretching and bending vibrations[15–19] signaled the power of this new technique. Similarly, near-infrared combination bands built on the monomer stretching fundamental have provided detailed information on the vibrationally excited monomer potential surface for several of the rare-gas–hydrogen halide complexes.[20] More recently, tunable FIR spectra of ArH_2O have been directly fit to an accurate three-dimensional potential-energy surface,[21] and an effective angular potential-energy surface for $ArNH_3$ has been determined from FIR vibration–rotation–tunneling (VRT) measurements,[22] indicating the generality of this approach.

Hutson, Beswick, and Halberstadt[23] explored the potential of such techniques for the determination of three-body effects on intermolecular forces in a theoretical study of Ar_2HCl. Chosen as an ideal system for study because the pair potentials are very accurately known (Ar–Ar and Ar–HCl), the spectroscopic properties of Ar_2HCl were shown to be very sensitive to the subtle changes in the potential

 0021-9606/91/173182-09$03.00

expected from the influence of three-body forces.[23] This paper is the second in our continuing study of the Ar_2HCl system.[24] Our goal is to fully characterize the spectroscopically accessible states of Ar_2HCl with far-infrared vibration–rotation–tunneling laser spectroscopy and thus ultimately determine a full experimental intermolecular potential-energy surface, including three-body effects. However, as the following account will detail, the considerable complexity of the *dynamical* problem poses a severe additional challenge which must be overcome in order to realize the possibility of determining many-body effects on intermolecular forces through VRT spectroscopy.

EXPERIMENT

The Berkeley tunable far-infrared laser spectrometers have been described in detail previously,[19,25] and a general review of these devices has recently appeared.[26] Tunable far-infrared radiation is generated by mixing the output of an optically pumped fixed-frequency far-infrared laser with that of a continuously tunable microwave synthesizer in a Schottky barrier diode to produce radiation at the sum and difference frequencies ($\nu = \nu_{FIR} \pm \nu_{MW}$). The tunable sideband radiation is separated from the much stronger fixed-frequency carrier with a polarizing Michelson interferometer and then directed to multipass optics enclosing the supersonic jet expansion. The detected radiation intensity is monitored by second derivative lock-in detection.

In this particular study, the 262 μm CH_2F_2 and 272 μm CH_2DOH (1145.4302 and 1101.1594 GHz, respectively) laser lines provided the fixed-frequency radiation. The tunable radiation is detected by an InSb hot-electron bolometer configured in the "Putley mode" (a fixed 5 kG magnetic field), as in our previous study of Ar_2HCl. Atmospheric water absorptions pose a particularly acute problem in this area of the FIR spectrum. Although the entire beam path is purged with dry nitrogen, the laser power on the detector was noted to vary with the day-to-day change in humidity in our laboratory. Multipass optics are employed to direct the FIR radiation through the planar jet with 10 passes.[27,28]

The $Ar_m(HCl)_n$ clusters were generated by continuously expanding a mixture of Ar and HCl through a 10 cm $\times$ 25 μm planar jet into a vacuum chamber evacuated by a 2500 cubic feet per minute Roots pump system. As in our previous study, we found an optimum HCl/Ar mix of $\sim$0.5% and an optimum chamber operating pressure of $\sim$300 mTorr. Previously, we reported that the cooling of our nozzle (to -78 °C) resulted in a twofold increase in Ar_2HCl signal strength.[24] It now appears that the spacing between faceplates on the nozzle is the most critical factor influencing Ar_2HCl cluster production. If the faceplates are set to the smallest spacing possible ($\sim$25 μm), cooling of the nozzle does *not* result in an increase in signal. Thus, we suspect that the effect we observed previously was due to mechanical changes in the nozzle upon cooling rather than actual cooling of the gas mixture prior to expansion.

RESULTS AND ANALYSIS

The present VRT band was observed upon continuous scanning to lower frequency from the position of the previously reported band. We have now continuously scanned the region 36–41 cm^{-1} for Ar_2HCl spectra. Although intensity information is not very reliable due to varying laser power, we estimate, taking sensitivity considerations into account, that the present band is at *least* a factor of 3 times more intense than the band we reported previously.

Rotational assignment

The Ar_2HCl ground-state geometry corresponds to an asymmetric top T-shaped configuration resulting in a C_{2v} symmetry axis along the Ar_2–HCl van der Waals bond. Because rotation about this axis involves exchange of identical boson nuclei (^{40}Ar; $I = 0$), the total wave function must be symmetric with respect to this motion. Additionally noting that the C_{2v} symmetry axis has the smallest moment of inertia of the three principal axes, it is seen that K_p quantum number must possess only even values in the ground state.

Because Ar_2HCl is a large asymmetric top and both the chlorine-35 and -37 isotopes are spectroscopically observable in natural abundance, the rotational structure was extremely dense and thus was difficult to assign. We resorted to a three-step computer-intensive process to assign the observed frequencies. First, the transitions were sorted into patterns that reflected the approximate rotational spacing expected for Ar_2HCl. Second, combination differences were calculated from the ground-state constants determined in our previous simultaneous microwave–FIR fit,[24] providing accurate frequencies for up to $J = 15$ levels. Third, transitions from the sorted patterns were matched via combination differences to other patterns (e.g., and R-branch pattern would be linked to a P- or Q-branch pattern). This process was performed successfully for both Ar_2HCl isotopes and led to absolute quantum number assignments for the ground-state levels of each transition. The absolute assignment of the upper-state levels still relied on the assumed symmetry of the vibrational motion.

The symmetry of the vibrational motion also proved difficult to assign. Based on the combination difference analysis, c-type symmetry could be ruled out because c-type selection rules could not connect the states identified by combination differences. However, to differentiate between an a-type and a b-type transition requires knowledge of the change in the K_p quantum number. Although nuclear-spin statistics forbid the existence of the K_p = odd member of an asymmetry doublet in the ground state, there still exists an ambiguity in the upper-state level. Due to the fact that Ar_2HCl is a near oblate symmetric top ($\kappa = 0.85$), the asymmetry splitting (the energy separation between $J_{K_pK_Q}$ and $J_{K_p \pm 1K_Q}$ levels) is less than the accuracy of our FIR laser spectrometer (< 1 MHz). For example, a transition involving the ground-state level 3_{21} would occur at the same experimentally resolved frequency whether the upper-state level was 4_{32} (a b-type transition) or 4_{22} (an a-type transition). Therefore, equally well-fit spectroscopic constants could be obtained with either assignment. In our previous analysis, we were able to assign that vibrational transition as a type because we observed a $P(1)$ and a $R(0)$ transition originating from the $K_p = 0$ ground-state subband. Since we

have established that the present band must be either *a* or *b* type, the existence of a similar $P(1)$ transition would provide the information needed for the assignment. However, neither $P(1)$ nor $P(2)$ were observed in this instance, indicating that the experimental sensitivity does not allow the vibrational assignment to be made on this basis. Alternatively, the existence of Q-branch transitions to upper-state levels of the form J_{J0} directly indicate *b*-type vibrational symmetry for Ar_2HCl. For example, the upper-state level 7_{70} (which is not asymmetry doubled) can only be connected via a Q-branch transition to the lower-state levels 7_{71} and 7_{61}. Since K_p = odd ground-state levels are forbidden, any observed transition occurring at this frequency must be due to a $7_{70} \leftarrow 7_{61}$ transition. We have observed $Q(1)$, $Q(3)$, $Q(5)$, $Q(7)$, and $Q(9)$ transitions of this form for $Ar_2H\,^{35}Cl$ and therefore assign the observed band as being of *b*-type symmetry. The observed transitions are recorded in Table I.

Most of the assigned transitions appeared as doublets, due to nuclear hyperfine interactions, and their line centers were taken to be simply the average of the two doublet components. These line centers were used in a fit of the data to a Watson *S*-reduced Hamiltonian.[29] The ground-state constants were held fixed to the values determined in the previous microwave–FIR analysis, as the present data did not access additional ground-state levels. Band origins, rotational constants, and quartic distortion constants for this VRT band were determined for both $Ar_2H\,^{35}Cl$ and $Ar_2H\,^{37}Cl$ and are listed as state $|2\rangle$ in Table II.

Axis switching

Because the displacement of the nuclear coordinates upon vibrational excitation is essentially the same for both Ar_2HCl isotopes, it is reasonable to expect the percent change in the rotational constants upon vibrational excitation to be about the same for both isotopes as well. Assuming that this criterion holds, the observation of two isotopes provides a check for internal consistency of the total rotational assignment. In our previous analysis, this criterion directly led to the *assignment* of the $Ar_2H\,^{37}Cl$ spectrum. Therefore, to reconcile the rotational constants determined in this analysis for the two isotopes requires that the $Ar_2H\,^{35}Cl$ isotope exhibits an "axis-switching" transition while the $Ar_2H\,^{37}Cl$ isotope does not (Table III). The use of the principal axes (defined by the relative ordering of the moments of inertia) to define a molecule-*fixed* axis system is only rigorous for small nuclear displacements. If the displacement occurring upon excitation is large enough, the relative ordering of the moments of inertia can change, and thus the principal axes can be rotated with respect to the molecular geometry. This is termed an axis-switching transition. Axis switching has been studied in connection with electronic transitions, wherein the nuclear displacement can be quite large, but it is

TABLE I. Observed frequencies and residuals (MHz) for the VRT band of Ar_2HCl observed in this work.

$J'_{K_pK_o}$	$J''_{K_pK_o}$	$\nu(Ar_2H\,^{35}Cl)$	O–C	$\nu(Ar_2H\,^{37}Cl)$	O–C
14_{114}	15_{015}	1 085 554.4	−1.0		
13_{113}	14_{014}	1 087 652.1	−0.5		
12_{112}	13_{013}	1 089 730.9	−0.4	1 089 800.8	0.5
11_{111}	12_{012}	1 091 791.9	2.7	1 091 817.3	1.8
10_{110}	11_{011}	1 093 825.1	1.0	1 093 808.4	0.3
9_{19}	10_{010}	1 095 834.8	0.8	1 095 775.8	−0.4
8_{18}	9_{09}	1 097 816.9	−0.2	1 097 717.3	−0.9
5_{15}	6_{06}	1 103 589.1	−0.6		
4_{14}	5_{05}	1 105 449.9	−0.8	1 105 196.4	0.9
3_{13}	4_{04}	1 107 278.1	−0.2		
2_{12}	3_{03}	1 109 071.2	−1.2		
1_{10}	1_{01}	1 115 952.8	0.0		
3_{12}	3_{03}	1 119 168.2	1.6		
4_{13}	4_{04}	1 120 741.3	−0.4		
7_{16}	7_{07}	1 125 259.3	−0.8		
8_{17}	8_{08}	1 126 702.3	−1.1		
2_{12}	1_{01}	1 119 257.4	−2.3		
3_{13}	2_{02}	1 120 812.0	−1.1		
4_{14}	3_{03}	1 122 359.7	−0.6	1 121 786.7	1.3
5_{15}	4_{04}	1 123 874.6	−0.9	1 123 274.0	0.1
6_{16}	5_{05}	1 125 357.3	−0.6	1 124 730.2	−0.8
7_{17}	6_{06}	1 126 807.9	−0.5	1 126 155.8	−1.3
8_{18}	7_{07}	1 128 228.0	−0.2	1 127 553.0	−0.4
9_{19}	8_{08}	1 129 618.7	0.0	1 128 920.0	−1.2
10_{110}	9_{09}	1 130 982.1	0.7	1 130 261.2	−0.7
11_{111}	10_{010}	1 132 320.6	2.4	1 131 578.2	1.0
12_{112}	11_{011}	1 133 631.6	0.8	1 132 871.2	2.3
13_{113}	12_{012}	1 134 920.4	−1.1	1 134 139.2	0.3
14_{114}	13_{013}	1 136 190.7	−1.8	1 135 389.5	0.1

TABLE I. (*Continued.*)

$J'_{K_a K_c}$	$J''_{K_a K_c}$	$\nu(Ar_2H\,^{35}Cl)$	O–C	$\nu(Ar_2H\,^{37}Cl)$	O–C
15_{115}	14_{014}	1 137 443.8	−2.4	1 136 621.9	−0.7
16_{116}	15_{015}	1 138 686.6	1.4		
13_{112}	14_{213}	1 085 988.8	3.7		
12_{111}	13_{212}	1 088 060.6	3.2		
11_{110}	12_{211}			1 090 182.9	−1.1
10_{19}	11_{210}	1 092 139.5	0.0	1 092 169.5	−0.7
9_{18}	10_{29}	1 094 144.5	−0.6	1 094 132.3	−0.4
8_{17}	9_{28}	1 096 123.8	−0.5	1 096 070.2	0.5
7_{16}	8_{27}	1 098 974.3	−0.7		
5_{15}	6_{24}	1 096 495.1	−1.3		
4_{13}	5_{24}	1 103 747.1	0.2		
3_{12}	4_{23}	1 105 572.7	2.9		
1_{10}	2_{21}	1 109 016.5	−1.3		
2_{12}	2_{21}	1 112 328.8	3.2		
3_{12}	3_{21}	1 112 513.3	2.6		
4_{14}	4_{23}	1 108 765.3	1.8		
4_{13}	4_{22}	1 110 521.2	0.7		
5_{14}	5_{23}			1 108 340.6	1.1
12_{112}	12_{211}	1 092 872.9	−2.8		
3_{12}	2_{21}	1 122 419.7	0.7		
4_{13}	3_{22}	1 124 068.3	−0.6		
5_{14}	4_{23}	1 125 592.0	−1.4	1 124 968.5	0.7
6_{15}	5_{24}	1 127 076.5	−0.8	1 126 429.0	0.0
7_{16}	6_{25}	1 128 528.9	−0.4	1 127 857.4	0.0
8_{17}	7_{26}	1 129 950.1	−1.0	1 129 256.4	−0.2
9_{18}	8_{27}	1 131 344.5	−0.6	1 130 628.4	0.5
10_{19}	9_{28}	1 132 711.3	1.7		
11_{110}	10_{29}	1 134 051.8	2.0		
12_{111}	11_{210}			1 134 589.3	−1.1
13_{112}	12_{211}			1 135 865.1	−2.0
12_{310}	13_{211}	1 086 387.6	3.0	1 086 550.6	−0.2
11_{39}	12_{210}	1 088 431.3	0.0	1 088 552.3	−0.5
10_{38}	11_{29}	1 090 455.3	−1.0	1 090 534.1	0.1
9_{37}	10_{28}	1 092 456.1	−1.4	1 092 492.6	0.4
8_{36}	9_{27}	1 094 431.4	−1.6		
8_{35}	9_{28}	1 116 645.4	2.6		
7_{35}	8_{26}	1 096 380.1	−0.9		
3_{30}	3_{21}	1 115 941.2	−3.7		
4_{32}	4_{23}	1 119 035.4	−3.9		
5_{33}	5_{24}	1 120 574.5	1.3	1 120 044.8	−1.5
6_{33}	6_{24}	1 120 377.6	3.4		
6_{34}	6_{25}	1 122 080.6	0.9		
7_{34}	7_{25}	1 121 852.8	1.9	1 121 325.6	2.2
8_{35}	8_{26}	1 123 296.5	0.3		
8_{36}	8_{27}	1 124 997.9	−0.7		
9_{37}	9_{28}	1 126 413.9	−0.7		
9_{36}	9_{27}	1 124 711.4	−1.1		
13_{310}	13_{211}			1 129 474.6	1.2
5_{33}	4_{22}	1 127 346.9	0.1	1 126 796.1	0.0
6_{34}	5_{23}	1 128 800.5	0.3		
7_{35}	6_{24}	1 130 248.8	−1.3	1 129 566.8	0.6
8_{36}	7_{25}	1 131 672.7	0.0	1 130 963.8	0.5
9_{37}	8_{26}	1 133 067.7	0.6	1 132 336.9	1.6
10_{38}	9_{27}	1 134 434.8	0.0	1 133 682.1	0.1
11_{39}	10_{28}	1 135 779.0	1.4	1 135 004.4	−0.6
12_{310}	11_{29}	1 137 101.4	3.9	1 136 305.3	−0.6
11_{38}	12_{49}	1 086 752.5	−2.0	1 137 585.8	−1.1
10_{37}	11_{48}	1 088 771.9	−3.0		
9_{36}	10_{47}	1 090 769.3	−2.7		
8_{35}	9_{46}	1 092 743.0	−1.0	1 092 790.0	−1.9
7_{34}	8_{45}	1 094 689.0	−0.1	1 094 695.4	−3.6

TABLE I. (*Continued.*)

$J'_{K_a K_c}$	$J''_{K_a K_c}$	$\nu(Ar_2H\,^{35}Cl)$	O–C	$\nu(Ar_2H\,^{37}Cl)$	O–C
6_{33}	7_{44}	1 096 607.4	2.6		
4_{32}	4_{41}	1 111 842.9	−0.1		
5_{33}	5_{42}	1 110 284.2	1.4	1 109 867.2	−0.5
6_{34}	6_{43}	1 108 419.7	0.1	1 108 155.0	3.0
6_{33}	6_{42}	1 110 313.1	0.2		
7_{34}	7_{43}	1 108 239.1	−0.6	1 108 159.6	−3.6
11_{39}	11_{48}	1 098 446.3	−4.5		
13_{311}	13_{410}	1 094 300.8	−3.0		
13_{310}	13_{49}	1 096 060.3	1.5		
7_{34}	6_{43}	1 131 971.6	1.1	1 131 259.1	−3.7
8_{35}	7_{44}	1 133 395.6	−0.3	1 132 681.3	−0.7
9_{36}	8_{45}	1 134 788.9	−1.5		
10_{37}	9_{46}	1 136 157.8	−1.1	1 135 396.4	−0.5
11_{38}	10_{47}	1 137 503.3	0.0		
12_{39}	11_{48}	1 138 828.4	3.0	1 138 023.2	2.3
12_{310}	11_{47}	1 109 826.2	−0.5		
13_{310}	12_{49}			1 139 304.8	1.1
9_{55}	10_{46}	1 089 087.4	−2.4		
8_{54}	9_{45}	1 091 059.2	−0.1		
5_{50}	5_{41}	1 115 938.6	3.7		
6_{52}	6_{43}			1 118 239.6	−0.6
8_{54}	8_{45}	1 121 599.9	3.0		
9_{55}	9_{46}	1 123 015.1	0.7		
10_{55}	10_{46}	1 122 713.2	1.2		
11_{56}	11_{47}	1 124 077.3	−1.5		
11_{57}	11_{48}	1 125 768.8	−1.3		
12_{57}	12_{48}	1 125 420.8	−2.0		
12_{58}	12_{49}	1 140 552.9	0.4		
5_{51}	4_{40}	1 130 912.1	−4.4		
7_{53}	6_{42}	1 133 860.4	0.7		
8_{54}	7_{43}	1 135 147.8	0.3		
9_{55}	8_{44}	1 136 520.4	−0.1		
10_{56}	9_{45}	1 137 884.0	−1.5		
11_{57}	10_{46}			1 138 446.4	0.1
10_{55}	11_{66}	1 085 419.7	−2.4	1 085 695.1	3.0
9_{54}	10_{65}	1 087 415.4	2.1		
6_{52}	7_{61}	1 088 845.3	−0.5		
6_{52}	6_{61}	1 111 072.6	2.1	1 109 889.4	2.2
8_{54}	8_{63}	1 107 979.3	1.4		
10_{55}	9_{64}	1 139 619.6	−0.3		
11_{56}	10_{65}	1 140 959.4	−1.7		
12_{57}	11_{66}	1 142 279.9	−2.4		
9_{73}	10_{64}	1 085 767.2	1.9		
7_{70}	7_{61}	1 115 920.0	0.3		
7_{71}	7_{62}	1 117 132.2	2.1		
8_{72}	8_{63}	1 118 274.5	1.0		
11_{75}	11_{66}	1 122 394.4	1.6		
12_{75}	12_{66}	1 122 063.7	3.2		
12_{76}	12_{67}	1 123 737.4	−0.7	1 123 274.0	1.1
14_{77}	14_{68}	1 124 697.6	1.3		
14_{78}	14_{69}			1 125 844.4	−1.4
10_{73}	9_{64}			1 152 199.4	0.0
12_{75}	11_{66}	1 162 705.9	−1.7		
8_{72}	8_{81}	1 109 992.7	−1.4		
10_{73}	9_{82}			1 141 150.2	3.0
9_{90}	9_{81}	1 115 870.6	−0.2		
10_{91}	10_{82}			1 116 976.6	−0.4
12_{94}	12_{85}			1 120 155.5	−1.9
15_{97}	14_{86}	1 151 373.8	−0.7		
11_{111}	11_{102}	1 116 297.5	−0.1		
15_{115}	15_{106}	1 121 032.4	0.6		

TABLE II. Molecular constants (MHz) determined from a least-squares fit to all observed spectra for Ar_2HCl. Stated uncertainties are one standard deviation. See text for explanation of column notation.

	$Ar_2H\ ^{35}Cl$			$Ar_2H\ ^{37}Cl$		
	$\|0\rangle$	$\|1\rangle$	$\|2\rangle$	$\|0\rangle$	$\|1\rangle$	$\|2\rangle$
ν_0		1 185 820.7(3)	1 115 098.6(2)		1 185 506.9(4)	1 114 653.4(4)
B_x	1 733.8560(4)	1 730.70(4)	1 666.77(4)	1 733.824 7(4)	1 731.33(4)	1 669.92(4)
B_y	1 667.921 40(18)	1 720.89(3)	1 699.73(4)	1 606.865 1(5)	1 663.62(4)	1 634.21(3)
B_z	844.448 7(16)	883.040(13)	826.693(6)	828.456 42(16)	867.73(2)	811.239(10)
D_J	0.024 201(7)	0.017 47(13)	0.013 52(3)	0.023 369(14)	0.019 5(2)	0.016 63(9)
D_{JK}	− 0.040 915(18)	− 0.104 4(10)	− 0.386 2(11)	− 0.039 33(4)	− 0.010 6(3)	− 0.046 86(19)
D_K	0.018 679(14)	0.002 74(19)	0.019 67(9)	0.017 83(3)	0.001 5(2)	0.025 26(12)
d_1	0.002 479(6)	− 0.001 98(17)	− 0.001 06(17)	0.002 927(17)	0.004 6(2)	
d_2	− 0.000 406 6(18)	− 0.002 18(5)	− 0.000 54(13)	− 0.000 456(6)	− 0.003 55(7)	
χ_{xx}	− 28.123(14)	− 19.69(19)	− 23.2(4)	− 22.201(5)	− 14.9(5)	− 19(2)
χ_{yy}	12.471(13)	6.72(19)	4.8(4)	9.844(21)	5.3(5)	6(2)
χ_{zz}	15.658(13)	12.97(19)	18.38(9)	12.356(21)	9.7(2)	12.9(5)

clear that large-amplitude van der Waals vibrations could also easily cause axis switching. Twenty-six years ago Hougen and Watson invoked axis switching to explain the appearance of "forbidden" transitions in a 2400 Å system of acetylene. They showed that axis switching can result in the breakdown of the asymmetric top selection rules, leading to the observation of additional, albeit weak, transitions.[30] Due to the effects of nuclear-spin statistics on the upper-state levels and our inability to resolve the asymmetry doubling, we have not actually observed any axis-switching transitions. However, it is clear from the relative changes in the excited-state rotational constants (Table III) that the a and b axes have switched in the more nearly oblate $Ar_2H\ ^{35}Cl$ isotopomer. Therefore, we relabel the molecule-fixed axes as follows: x axis (ground-state a axis), along the Ar_2–HCl van der Waals bond; y axis (ground-state b axis), perpendicular to the x axis and parallel to the Ar–Ar axis; z axis (ground-state c axis), perpendicular to the x and y axes (Fig. 1).

Hyperfine analysis

As in our previous analysis,[24] the nuclear quadrupole coupling constants were determined in a separate least-squares fit with the line centers determined from the rotational fit. The first-order matrix elements for the nuclear quadrupole Hamiltonian were calculated in the coupled basis set $|JKIF\rangle$ ($F = I + J$; $I = 3/2$ for both ^{35}Cl and ^{37}Cl).[31] Because the nuclear quadrupole principal axes are chosen to coincide with inertial principal axes, the nuclear quadrupole coupling constants must be expressed in the new axis system as well. The upper-state nuclear quadrupole coupling constants (χ_{xx}, χ_{yy}, and χ_{zz}) were fit with the ground-state constants held at the values determined by Klots *et al.*[12] (Table IV). The overall rotational structure of the observed band is depicted in Fig. 2 and representative hyperfine structure is presented in Fig. 3.

Monomer orientation

In our previous analysis, we utilized the observation of two isotopes to establish the orientation of the HCl monomer in that excited vibrational state as being Ar_2ClH.[24] With use of the equation relating the planar moments to moments of inertia,

$$P_x = 1/2(I_y + I_z - I_x), \tag{1}$$

and neglecting torsional oscillations, the following expression is obtained:

$$P_x = \mu R^2 + I_{HCl}. \tag{2}$$

Here μ is the reduced mass of the complex, R is the distance

TABLE III. Percent change in vibrationally excited rotational constants from ground-state values for Ar_2HCl. Ground state: $A = B_x$, $B = B_y$, $C = B_z$, following the usual principal axis definition: $A > B > C$.

	$\|1\rangle$		$\|2\rangle$			
	$A = B_x$, $B = B_y$, $C = B_z$ for both isotopes (no axis switching)		$A = B_x$, $B = B_y$, $C = B_z$ for both isotopes (no axis switching)		$A = B_y$, $B = B_x$, $C = B_z$ for $Ar_2H\ ^{35}Cl$ (axis switching)	
	$Ar_2H\ ^{35}Cl$	$Ar_2H\ ^{37}Cl$	$Ar_2H\ ^{35}Cl$	$Ar_2H\ ^{37}Cl$	$Ar_2H\ ^{35}Cl$	$Ar_2H\ ^{37}Cl$
B_x	− 0.2	− 0.1	− 2.0	− 3.7	− 3.9	− 3.7
B_y	3.2	3.5	− 0.1	1.7	1.9	1.7
B_z	4.6	4.7	− 2.1	− 2.1	− 2.1	− 2.1

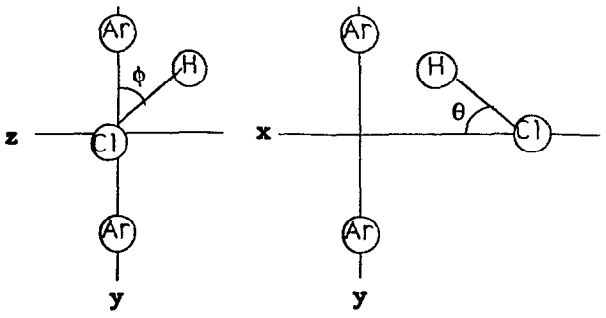

FIG. 1. Coordinate system for Ar_2HCl.

between the Ar_2 and HCl centers of mass, and I_{HCl} is the moment of inertia of HCl. In the ground state, R is 3.4969(1) Å for $Ar_2H\,^{35}Cl$ and 3.4675(1) Å for $Ar_2H\,^{37}Cl$. Klots *et al.* established that the ground-state equilibrium structure is oriented in the sense of Ar_2HCl because the center-of-mass separation is *smaller* for the ^{35}Cl isotope.[12] In our previous analysis we established the upper-state vibrationally averaged geometry as Ar_2ClH because the center-of-mass separation was *larger* for the ^{35}Cl isotope.[24] For the presently accessed vibrational state, R is 3.4838(4) and 3.4879(4) Å for $Ar_2H\,^{35}Cl$ and $Ar_2H\,^{37}Cl$, respectively, establishing the vibrationally-averaged geometry as Ar_2HCl.

DISCUSSION

In our first paper investigating the Ar_2HCl system, we interpreted the measured band in terms of an ArHCl-type energy-level diagram.[24] ArHCl possesses three low-frequency van der Waals vibrational modes: one stretching state and two bending states. The bending states are best thought of as correlating to free HCl rotation ($j=1$; $m_j=0,\pm1$). In ArHCl, the Ar atom breaks the degeneracy between the $m_j=\pm1$ and the $m_j=0$ states of HCl. Thus, the ArHCl bending states are referred to as a singly degenerate Σ bend ($m_j=0$) and a doubly degenerate Π bend ($m_j=\pm1$). Of course, Coriolis-induced l-type doubling can (and does in the ArHCl case) split the Π bend degeneracy. The Ar_2HCl trimer possesses additional vibrational modes due to Ar–Ar stretching and bending (the motion of the Ar–Ar axis relative to the Ar_2–HCl axis) motions. In addition, the presence of *two* Ar atoms completely destroys the HCl m_j degeneracy, leading to three distinct bending states. Hutson, Beswick, and Halberstadt refer to the state correlating to $m_j=0$ as the parallel bend (identical to the Σ bend of ArHCl) and the states correlating to $m_j=\pm1$ as the in-plane and out-of-plane bends (these states are related to the formerly degenerate π bend of ArHCl).[23] Although only transitions involving the HCl bending states are expected to carry much intensity in the FIR spectrum, the fact that all of these states are expected to lie between 30 and 45 cm^{-1} indicates that substantial mixing of vibrational states might be possible. Vibrational-state mixing is operative in the ArHCl system, manifesting itself in the nonzero transition moment of the van der Waals stretch. Consequently, an ArHCl-type energy-level diagram may provide only a zero-order description of the disposition of the vibrational eigenstates in the Ar_2HCl complex.

We assigned the first Ar_2HCl band observed to the parallel bend (or equivalently, Σ bend) for the following reasons: It was obvious from the excited-state rotational constants that the motion involved some bending coordinate. Second, the symmetry of the vibrational motion was determined to be a type, in accordance with a parallel bending coordinate, rather than a perpendicular one. Third, the hyperfine projections evidenced an increased bending amplitude and unhindered torsional motion for the HCl monomer in the excited state. Although increased bending amplitude would also be expected for the perpendicular bending states, the torsional motion would be expected to be localized in-plane or out-of-plane, depending on which bend was excited. Finally, the equilibrium orientation of the HCl monomer in this state was determined to be Ar_2HCl, as is the case for the parallel bend of ArHCl. It thus was established that this state behaved very much like the parallel bending state expected from an ArHCl-type energy-level diagram.

In the present band, the information extracted from an interial analysis is less straightforward. If torsional motion of the HCl monomer is neglected, the following expressions for the rotational constants are obtained:

$$B_x \approx \langle \hbar^2/2I_{Ar_2} \rangle, \tag{3}$$

$$B_y \approx \langle \hbar^2/2\mu R^2 \rangle, \tag{4}$$

$$B_z \approx \langle \hbar^2/(2\mu R^2 + 2I_{Ar_2}) \rangle \tag{5}$$

(where R is the vector between the Ar_2 and HCl centers of mass and μ is the pseudodiatomic reduced mass of the complex). Although this approximation results in quantitative disagreement with absolute experimental results, it is useful in understanding the contributions to the *relative* change in rotational constants. It is seen that the zero-order contribution to the B_x rotational constant is simply the distance between the Ar atoms. Since B_x decreases by nearly 4% upon excitation, it seems that the present band involves a substantial Ar–Ar motion, whereas the previous band showed insignificant change in this rotational constant (see Table III).

TABLE IV. Angular expectation values for all measured states of Ar_2HCl.

	$Ar_2H\,^{35}Cl$			$Ar_2H\,^{37}Cl$		
	$\|0\rangle$	$\|1\rangle$	$\|2\rangle$	$\|0\rangle$	$\|1\rangle$	$\|2\rangle$
$\langle P_2(\cos\theta)\rangle$	0.4165(4)	0.291(3)	0.343(6)	0.4166(1)	0.280(10)	0.36(4)
$\langle \Delta(\theta,\phi)\rangle$	0.0313(2)	0.062(7)	0.134(4)	0.0314(3)	0.055(15)	0.08(2)

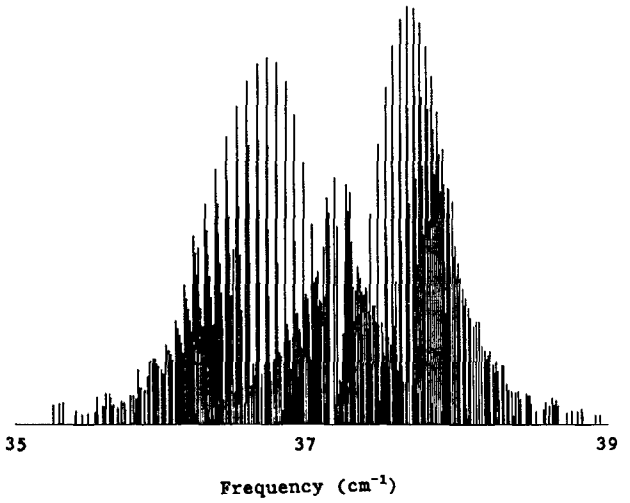

FIG. 2. Calculated stick spectrum of the presently measured Ar_2H ^{35}Cl vibration–rotation band ($T_r = 5$ °K).

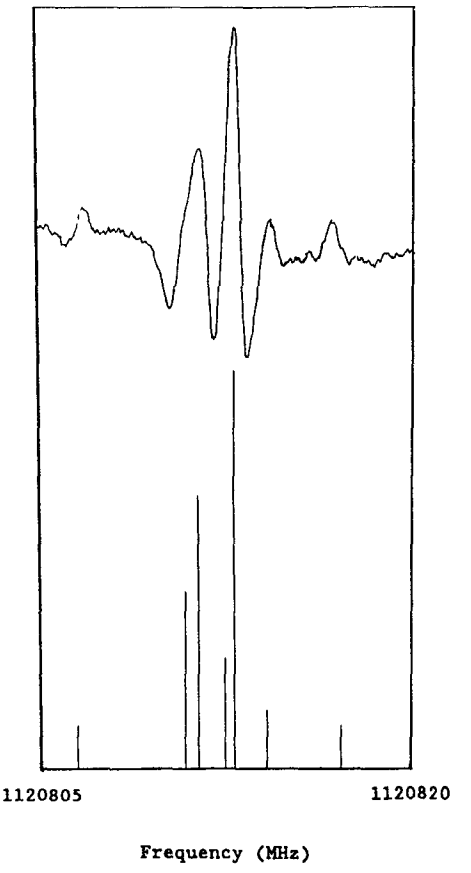

FIG. 3. Observed (top) and calculated (bottom) nuclear quadrupole hyperfine structure for the $2_{02} \rightarrow 3_{13}$ transition arising from the 37.2 cm^{-1} vibration–rotation band of Ar_2H ^{35}Cl.

Similarly, the value of the B_y rotational constant is dictated by the length of the Ar_2–HCl van der Waals bond. The present band indicates that this distance is shortened in the excited state, and that it is the combination of the change in the Ar–Ar and the Ar_2–HCl average bond lengths that leads to axis switching in Ar_2H ^{35}Cl. The B_z rotational constant measures the net effect of these motions. Because the calculated inertial defect ($\Delta = 10.797$ amu Å^2 for Ar_2H ^{35}Cl) is positive, the vibrational motion seems to be largely in-plane.

The present band was determined to be of *b*-type symmetry, indicating an in-plane perpendicular transition. Based on the rotational constant information and the symmetry of the vibrational motion, it would seem that the observed band is the in-plane bend (one of the two components of an ArHCl-type Π bend) coupled to an Ar–Ar stretching or bending motion. However, the measured hyperfine projections

$$\chi_{xx} = \chi_{HCl} \langle P_2 (\cos\theta) \rangle, \tag{6}$$

$$\chi_{yy} - \chi_{zz} = (\tfrac{3}{2}) \chi_{HCl} \langle \Delta(\theta,\phi) \rangle \tag{7}$$

[where χ_{HCl} is the quadrupole coupling constant of the uncomplexed HCl monomer and $\Delta(\theta,\phi) = \sin^2\theta \cos 2\phi$] indicate a more complicated picture. The deviation of $\langle P_2 (\cos\theta) \rangle$ from unity is a measure of the bending amplitude of the HCl monomer, while the deviation of $\langle \Delta(\theta,\phi) \rangle$ from zero characterizes the anisotropy of the torsional motion (positive values indicating in-plane localization and negative values indicating out-of-plane localization) of the HCl monomer. Therefore, the in-plane bend is expected to exhibit a value of $\langle P_2 (\cos\theta) \rangle$ near zero and a relatively large positive value for $\langle \Delta(\theta,\phi) \rangle$. The out-of-plane bend would similarly show $\langle P_2 (\cos\theta) \rangle$ to be near zero, but a relatively large negative value for $\langle \Delta(\theta,\phi) \rangle$. The parallel motions (parallel bend and stretch) would be expected to possess larger $\langle P_2 (\cos\theta) \rangle$ values (due to smaller bending amplitudes) and $\langle \Delta(\theta,\phi) \rangle$ values near zero (small torsional localization). It may be seen (Table IV) that the measured hyperfine projections are *not* consistent with the values expected for the in-plane bend. The hyperfine information indicates a state which has a similar bending amplitude and torsional anisotropy to the previously parallel bending state and also to that expected for the van der Waals stretch. Therefore, it is reasonable to assume that the present state may be a mixture of several states.

Consequently, it is appropriate to refrain from labeling the two excited Ar_2HCl states in an unperturbed ArHCl-type picture. We therefore label the presently measured states as follows: $|0\rangle$ is the ground state, $|1\rangle$ is the state that lies 39.5 cm^{-1} above $|0\rangle$, and $|2\rangle$ is the state that lies 37.2 cm^{-1} above $|0\rangle$. It is still clear that state $|1\rangle$ shows spectroscopic compliance with an unperturbed parallel bending state, but the present results suggest the possibility of mixing. It also seems appropriate to expect that the present mixed state is most dominated by the in-plane bending state, as this would explain the increased transition strength relative to $|1\rangle$, the change in the B_y rotational constant, and the symmetry of the vibration. However, additional states must be measured in order to reliably characterize the "pure state" contributions to the excited eigenstates of Ar_2HCl.

In their calculation of Ar_2HCl spectroscopic properties, Hutson, Beswick and Halberstadt employed the "reversed adiabatic" approximation in order to simplify the five-dimensional dynamical problem to a tractable one of three dimensions[23] In the case of Ar_2HCl, the reversed adiabatic

approximation was used to decouple the Ar–Ar bending and stretching motions from the HCl motions. Therefore, calculations were performed for fixed values of the Ar–Ar bending and stretching coordinates. In the interest of reducing a very formidable dynamics problem to one that is tractable, Hutson, Beswick, and Halberstadt employed this approximate method, although Hutson has already noted that such a drastic approximation may not be valid.[32] Indeed, the present work shows this approximation to be a poor one, as we have directly evidenced the coupling between the Ar–Ar and HCl coordinates. It is clear that a more complete theoretical dynamical calculation must be developed in order to address the interesting and important three-body interactions that operate in the Ar_2HCl system.

ACKNOWLEDGMENTS

This work was supported by the NSF Physical Chemistry Program (Grant No. CHE-8612296). The authors again wish to thank Ron Cohen and Charlie Schmuttenmaer for helpful discussions.

[1] G. C. Maitland, M. Rigby, E. B. Smith, and W. A. Wakeham, *Intermolecular Forces* (Clarendon, Oxford, 1981).
[2] N. R. Kestner and O. Sinanoglu, J. Chem. Phys. **38**, 1730 (1963).
[3] J. D. Johnson and M. L. Klein, Trans. Faraday Soc. **60**, 1964 (1964).
[4] J. A. Barker and D. H. Everett, Trans. Faraday Soc. **58**, 1608 (1962).
[5] B. M. Axilrod and E. Teller, J. Chem. Phys. **11**, 299 (1943).
[6] P. J. Kortbeek and J. A. Schouten, Mol. Phys. **69**, 981 (1990).
[7] G. Chalansinki, M. M. Szczesniak, and S. Scheiner, J. Chem. Phys. **94**, 2807 (1991).
[8] H. S. Gutowsky, T. D. Klots, C. Chuang, C. A. Schmuttenmaer, and T. Emilsson, J. Chem. Phys. **83**, 4817 (1985).
[9] H. S. Gutowsky, T. D. Klots, C. Chuang, C. A. Schmuttenmaer, and T. Emilsson, J. Chem. Phys. **86**, 569 (1987).
[10] H. S. Gutowsky, T. D. Klots, C. Chuang, J. D. Keen, C. A. Schmuttenmaer, and T. Emilsson, J. Am. Chem. Soc. **107**, 7174 (1985); **109**, 5633 (1987).
[11] T. D. Klots, C. Chuang, R. S. Ruoff, T. Emilsson, and H. S. Gutowsky, J. Chem. Phys. **87**, 4383 (1987).
[12] T. D. Klots, C. Chuang, R. S. Ruoff, T. Emilsson, and H. S. Gutowsky, J. Chem. Phys. **86**, 5315 (1987); T. D. Klots and H. S. Gutowsky, *ibid.* **91**, 63 (1989).
[13] K. I. Peterson, R. D. Suenram, and F. J. Lovas, J. Chem. Phys. **90**, 5964 (1989).
[14] J. M. Hutson, J. Chem. Phys. **89**, 4550 (1988).
[15] D. Ray, R. L. Robinson, D.-H. Gwo, and R. J. Saykally, J. Chem. Phys. **84**, 1171 (1986).
[16] R. L. Robinson, D. Ray, D.-H. Gwo, and R. J. Saykally, J. Chem. Phys. **87**, 5149 (1987).
[17] R. L. Robinson, D.-H. Gwo, D. Ray, and R. J. Saykally, J. Chem. Phys. **86**, 5211 (1987); R. L. Robinson, D.-H. Gwo, and R. J. Saykally, Mol. Phys. **63**, 1021 (1988); J. Chem. Phys. **87**, 5156 (1987).
[18] R. J. Saykally, Acc. Chem. Res. **22**, 295 (1989).
[19] K. L. Busarow, G. A. Blake, K. B. Laughlin, R. C. Cohen, Y. T. Lee, and R. J. Saykally, J. Chem. Phys. **89**, 1268 (1988).
[20] D. J. Nesbitt, Chem. Rev. **88**, 843 (1988).
[21] R. C. Cohen and R. J. Saykally, J. Phys. Chem. **94**, 7991 (1990).
[22] C. A. Schmuttenmaer, R. C. Cohen, J. G. Loeser, and R. J. Saykally, J. Chem. Phys. **95**, 9 (1991).
[23] J. M. Hutson, J. A. Beswick, and N. Halberstadt, J. Chem. Phys. **90**, 1337 (1989).
[24] M. J. Elrod, D. W. Steyert, and R. J. Saykally, J. Chem. Phys. **94**, 58 (1991).
[25] G. A. Blake, K. B. Laughlin, K. L. Busarow, R. C. Cohen, D. Gwo, C. A. Schmuttenmaer, D. W. Steyert, and R. J. Saykally, Rev. Sci. Instrum. **62**, 1701 (1991).
[26] G. A. Blake, K. B. Laughlin, K. L. Busarow, R. C. Cohen, D. Gwo, C. A. Schmuttenmaer, D. W. Steyert, and R. J. Saykally, Rev. Sci. Instrum. **62**, 1693 (1991).
[27] D. Kaur, A. M. de Souza, J. Wanna, S. A. Hammad, L. Mercorelli, and D. S. Perry, Appl. Opt. **29**, 119 (1990).
[28] C. A. Schmuttenmaer, R. C. Cohen, N. Pugliano, J. R. Heath, A. L. Cooksy, K. L. Busarow, and R. J. Saykally, Science **249**, 897 (1990).
[29] J. K. G. Watson, J. Chem. Phys. **46**, 1935 (1967).
[30] J. T. Hougen and J. K. G. Watson, Can. J. Phys. **43**, 298 (1965).
[31] H. P. Benz, A. Bauder, and Hs. H. Gunthard, J. Mol. Spectrosc. **21**, 156 (1966).
[32] J. M. Hutson (private communication).